Current Biology 19, 2037–2042, December 15, 2009 ©2009 Elsevier Ltd All rights reserved DOI 10.1016/j.cub.2009.10.028

Report

Visualization of Individual *Scr* mRNAs during *Drosophila* Embryogenesis Yields Evidence for Transcriptional Bursting

Adam Paré,[1,*] Derek Lemons,[1] Dave Kosman,[1] William Beaver,[2] Yoav Freund,[2] and William McGinnis[1,*]
[1]Section of Cell and Developmental Biology, Division of Biology, University of California, San Diego, La Jolla, CA 92093, USA
[2]Department of Computer Science and Engineering, University of California, San Diego, La Jolla, CA 92093, USA

Summary

The detection and counting of transcripts within single cells via fluorescent in situ hybridization (FISH) [1–6] has allowed researchers to ask quantitative questions about gene expression at the level of individual cells. This method is often preferable to quantitative RT-PCR [7–9], because it does not necessitate destruction of the cells being probed and maintains spatial information that may be of interest. Until now, studies using FISH at single-molecule resolution have only been rigorously carried out in isolated cells (e.g., yeast cells or mammalian cell culture). Here, we describe the detection and counting of transcripts within single cells of fixed, whole-mount *Drosophila* embryos via a combination of FISH, immunohistochemistry, and image segmentation. Our method takes advantage of inexpensive, long RNA probes detected with antibodies [10, 11], and we present novel evidence to show that we can robustly detect single mRNA molecules. We use this method to characterize transcription at the endogenous locus of the Hox gene *Sex combs reduced* (*Scr*), by comparing a stably expressing group of cells to a group that only transiently expresses the gene. Our data provide evidence for transcriptional bursting [2, 5, 12–16], as well for divergent "accumulation" and "maintenance" phases of gene activity at the *Scr* locus.

Results and Discussion

In early *Drosophila* embryos, the limits of Hox expression domains along the anterior-posterior axis are set by parasegmental boundaries. Parasegments are repeating units of cellular organization that make up the body plan of early embryos, and the Hox gene *Sex combs reduced* (*Scr*) displays dynamic differences in expression between parasegments 2 and 3 (PS2 and PS3) (Figure 1). Cells in PS2, which give rise to the posterior mouthparts, stably express *Scr* from early embryogenesis onward. Cells in ventral PS3, which contribute to the first thoracic segment, display a transient burst of *Scr* transcription during mid-embryogenesis (Figures 1C–1E) [17–19]. Thus, this system offers a convenient way to compare *Scr* transcriptional dynamics between stably and transiently expressing groups of cells in the same embryo, as well the opportunity to shed light on the expression of a crucial developmental regulator.

*Correspondence: apare@ucsd.edu (A.P.), wmcginnis@ucsd.edu (W.M.)

Detection and Counting of Single *Scr* Transcripts

At low magnification, fluorescent signals from a probe directed against *Scr* mRNAs have a "speckled" appearance (Figure 2A). At high magnification, most cytoplasmic signals are resolvable as ellipsoids of roughly uniform size (~250–300 nm diameter in x and y, Figure 2B). Although we believed we were visualizing single mRNA molecules [1–6, 20–22], it was possible that they instead represented mRNA aggregates (e.g., P bodies [23]). One method for demonstrating single-transcript fluorescent in situ hybridization (FISH) resolution is to show that a spatial shift exists between signals from two different probes targeted to adjacent regions of an mRNA [1, 4, 6], which should not be present if one is visualizing an aggregate of randomly oriented transcripts. Consistent with this, we observed a randomly oriented spatial shift between signals from probes directed against the coding region and the 3′ UTR of *Scr* (see Figure S1 available online). Another method to demonstrate single RNA molecule detection is to show that the fluorescence emitted by specific numbers of direct-labeled oligonucleotide probes bound at each locus is reproducible and predictable [1, 4, 22]. Although the long RNA probes used in this study offer a large increase in signal-to-noise ratios, compared with oligonucleotide probes, because they are indirectly labeled, the fluorescence they emit is more variable ([11] and data not shown). Therefore, we developed a different assay to test whether the punctate cytoplasmic signals represented single transcripts. Single transcripts should contain only a single binding site for a unique probe sequence. If two probes against the same sequence are labeled with different hapten tags and simultaneously hybridized to embryos, there should be competition between the two probes, and very low levels of association should be observed.

We tested for such competition by using two unfragmented probes complementary to the same 330 bp region of the *Scr* 3′ UTR, labeled with either digoxigenin or dinitrophenyl haptens (probes S1 and S2, respectively; Figure 2H). This experiment was done as part of a triple hybridization, with a biotin-labeled coding region probe (ORF; Figure 2H) as a marker for the adjacent *Scr* mRNA protein-coding region (Figures 2D–2G). Randomly chosen S1 signals were almost always associated with an ORF signal (79%; n = 100; Figures 2D, 2E, and 2I), but rarely with an S2 signal (17%; n = 100; Figures 2E, 2F, 2G, and 2I). A given S1 signal was only associated with both an S2 and an ORF signal in a minority of cases (10%; n = 100; Figure 2I), which is strong evidence that these locations contain only single binding sites for an S probe. Although the S1 → S2 association statistics may seem high, rotating the S2 image stack 90° relative to the S1 image stack, and rescoring the same 100 S1 signals (to simulate random association) yields a nearly identical association level of 20% (Figure 2I), indicating that this association can be explained by the chance overlap of numerous signals in a finite volume. We therefore conclude that the large majority of the cytoplasmic *Scr* signals we observe correspond to single mRNA molecules. More pairwise association data, as well as antibody detection and probe binding efficiency data, are shown in Figures S1 and S2.

To group and count transcripts from single cells of the embryo, we used a combination of RNA FISH, immunohistochemistry

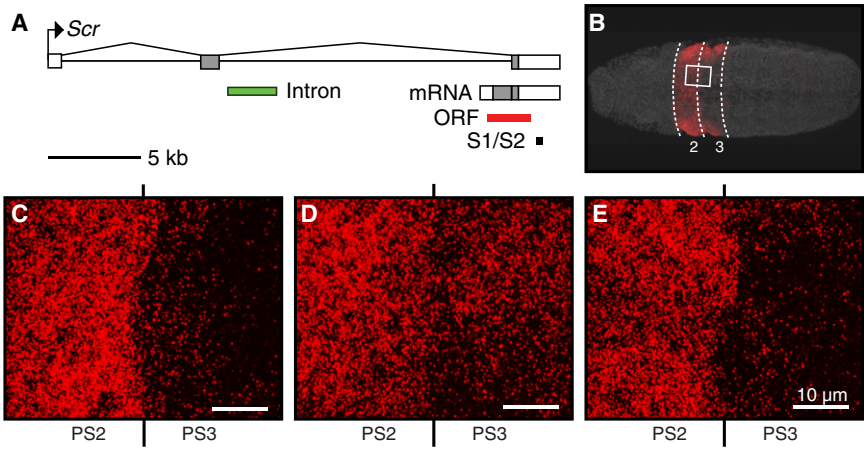

Figure 1. The *Scr* Expression Pattern During Midembryogenesis

(A) The *Scr* genomic locus, mRNA, and the locations of in situ probes used in this study.

(B) A ventral view of a stage 11 *Drosophila* embryo showing *Scr* mRNA (red) and nuclei stained with DAPI (gray). The boundaries of parasegments 2 and 3 (PS2 and PS3) are indicated with dashed lines. The white box highlights the approximate areas shown in (C)–(E).

(C–E) Expanded views of the area marked in (B) showing the boundary between PS2 and PS3 for a stage 10 embryo (C), an early stage 11 embryo (D), and a late stage 11 embryo (E). Transcripts are detected via FISH with a probe specific to the coding region of *Scr* (ORF probe). A high accumulation of *Scr* transcripts in PS2 is maintained throughout the three stages, whereas PS3 cells only highly accumulate *Scr* during early stage 11.

to detect cell boundaries, manual cell segmentation, and automated transcript signal segmentation. Cells of interest were manually segmented, with an anti-spectrin antibody [24] used to stain cell membranes as a guide. The cell segmentation process was accelerated with an ImageJ plugin we developed that allows a user to quickly draw unique regions of interest (ROIs) for each cell outline in a sequence of confocal image slices (Figures 3A and 3B). These ROIs then defined the 3D boundaries used to group the FISH signals from each cell (Figure 3C).

The punctate FISH signals themselves were automatically segmented and counted with the Volocity 3D image analysis program (Figure 3D). Almost all FISH transcript signal segmentations appeared correct upon visual inspection, and the algorithm yielded transcript counts that were nearly identical (±6%) to those obtained by manual counting (Table S1). Given

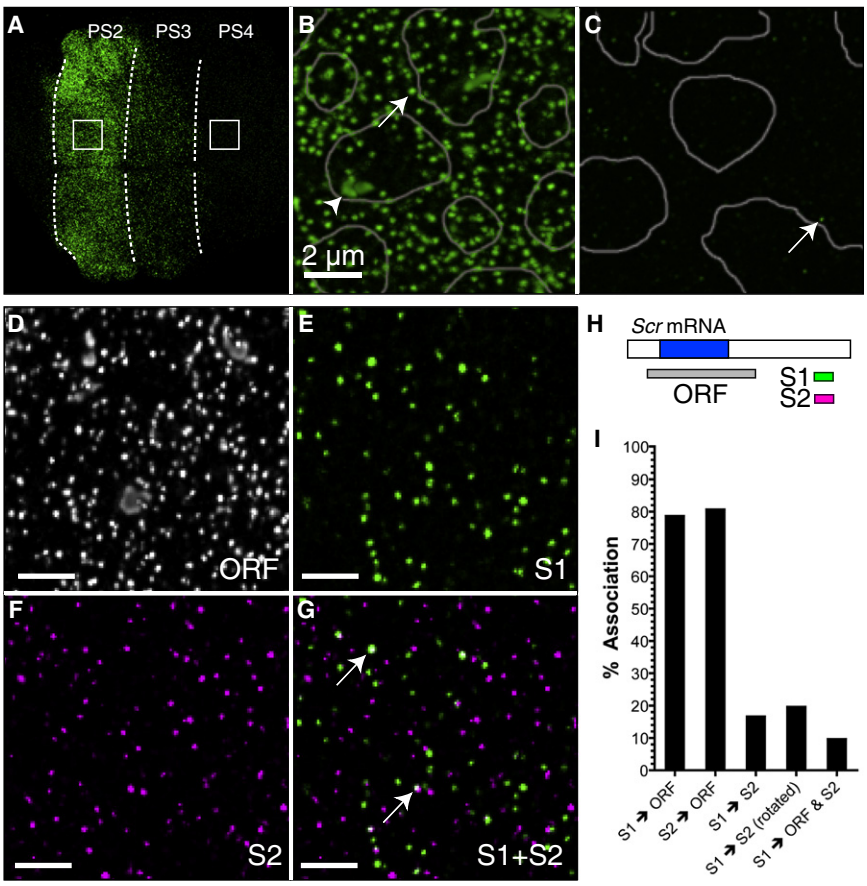

Figure 2. Competition for Binding Sites Demonstrates that Punctate Signals Represent Single mRNA Transcripts, and Not Groups of Transcripts

(A) A ventral view of *Scr* transcript expression during early stage 11. Parasegmental boundaries are indicated with dashed lines. A region with high transcript levels, and a region not expressing *Scr*, are marked with white boxes and are shown at high magnification in (B) and (C).

(B) *Scr* FISH signals are punctate (arrow). Sites of nascent transcription appear as large, often irregularly shaped, nuclear signals (arrowhead). Nuclear boundaries are based on DAPI staining and are indicated with gray lines.

(C) Areas outside the region of *Scr* expression sometimes contain very weak fluorescent signals (arrow), which are also seen with no probe controls (see also Figure S1).

(D–F) Results from a triple-hybridization "competition assay." FISH was carried out with the *Scr* ORF probe (D) and two differentially labeled unfragmented probes (S1 and S2) both complementary to the same region of the 3′ UTR (E and F).

(G) A merge of (E) and (F) shows very little colocalization between the competing S1 and S2 probes. Most associated signals (arrows) can be attributed to sites of nascent transcription, where multiple RNAs are present in a small volume.

(H) The *Scr* mRNA and the locations of FISH probes used in this assay.

(I) A histogram summarizing the pairwise associations between signals in the three fluorescent channels. "Association" is defined as significant overlap between signals in three dimensions. For example, the "S1 → ORF" bar refers to the percentage of time that an S1 signal overlaps with a signal from the ORF channel. "S1 → S2 (rotated)" refers to a control where an image stack from the S2 channel was rotated 90 degrees relative to the S1 channel, to simulate random association of signals. "S1 → ORF & S2" refers to cases of association in all three channels.

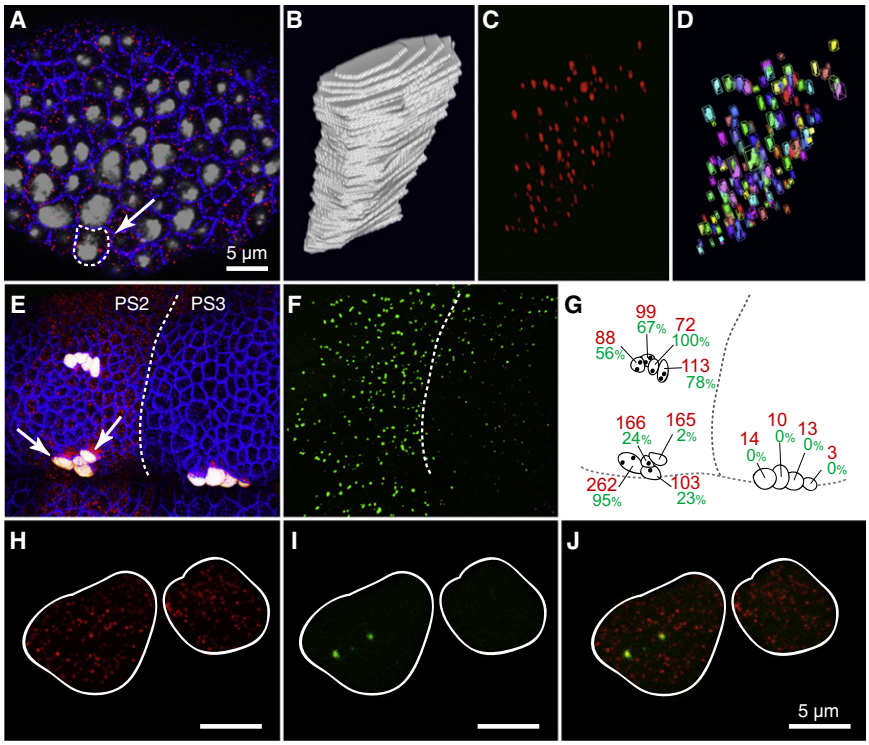

Figure 3. A Combination of Manual and Automated Image Segmentation Allows for Counting Transcripts within Individual Cells in Complex Tissues

(A) An image of *Scr*-expressing cells in a region of PS2 from a stage 11 embryo. Cell membranes are marked by spectrin staining (blue), nuclei are marked with DAPI (gray), and *Scr* transcripts are shown in red (ORF probe, Figure 1A). The segmented cell shown in (B–D) is indicated with a dashed line and arrow.

(B) A surface rendering of the volume defined by manual segmentation for the cell highlighted in (A).

(C) *Scr* probe signals from the segmented cell in (B).

(D) A false-color rendering of the signals in (C), which were segmented into individual objects.

(E) An image of *Scr*-expressing cells (ORF probe, Figure 1A) in PS2 and PS3 from a late stage 11 embryo. Cell membranes are marked by spectrin staining (blue), *Scr* transcripts are shown in red, and segmented cells are depicted as solid white objects. The pair of cells highlighted in (H–J) is indicated with arrows, and the boundary between PS2 and PS3 is marked with a dashed line.

(F) Nascent transcription detected with an intronic probe (Intron probe, Figure 1A) in the same embryo as shown in (E).

(G) A schematic showing *Scr* transcript numbers and relative nascent transcription strength for three groups of cells. Red numbers represent total transcripts per cell, and green numbers represent strength of nascent transcription (as the percentage of maximal intensity). Sites of nuclear transcription are represented as dots inside each cell.

(H–J) A pair of neighboring cells with identical transcript concentrations exhibiting divergent transcriptional states; shown are *Scr* transcripts (H), nascent transcription (I), and a merge of (H) and (I) (in J).

this variation and the fact that more than one transcript will occasionally occupy the same volume, we believe this counting method yields transcript numbers that are within ±10% of the actual value.

Analysis of *Scr* Transcription

Intense FISH signals representing sites of transcription in the nucleus are often detected with probes to upstream exons or introns of a gene (e.g., Figure 2B, arrowhead) [25, 26]. The transcriptional activity of a gene can be roughly quantified by measuring the fluorescence intensity of these spots, which will vary according to the number of nascent transcripts associated with the locus [1, 2, 5, 13, 27]. To characterize transcription at the *Scr* locus, we counted cytoplasmic transcripts with an ORF probe (Figure 3E) and nascent transcript intensity with an *Scr* intron probe (Figures 1A and 3F).

We first examined several stably expressing cells from PS2, as well as several transiently expressing cells in PS3 (Figures 3E and 3G). To our surprise, cell groups from both PS2 and PS3 displayed a wide range of cellular transcript numbers (72–262 for PS2, and 3–14 for PS3; Figure 3G). In PS3 cells, the low number of cytoplasmic transcripts was consistent with undetectable levels of nuclear transcription in the same nuclei. However, in PS2, there was not a good correspondence between cytoplasmic and nascent transcript signals; an extreme example of this is shown for two nearby cells (Figure 3E, arrows, and Figures 3H, 3I, and 3J). Although both cells contain over a hundred cytoplasmic mRNAs, one cell has two obvious sites of transcription, whereas the other has none.

To investigate this further, we carried out a more comprehensive analysis on three embryos during stages 10 and 11 of embryogenesis [28], and the results are shown in Figure 4. Embryos were chosen that were representative of different phases of *Scr* transcription: before, during, and after the transient period of *Scr* expression in PS3 (Figures 4A–4C). Approximately 20 ventro-lateral ectodermal cells from both PS2 and PS3 were segmented, and all cells were located ~50 μm from the ventral midline (Figures 4A–4F). Strongly expressing PS2 cells had an average of 94 mRNAs per cell, with the values exhibiting a large range from 33 to 177 mRNAs per cell (n = 58; Figure 4G). Differences in cell size were not responsible for this heterogeneity, because a similar distribution of values was seen after taking cell volume into account (Figure 4H). For each of the three stages examined, the average number of *Scr* transcripts per cell in PS2 was similar (100, 104, and 80). For PS3 cells, average *Scr* mRNA numbers were very low during stage 10 (5 transcripts), increased dramatically during early stage 11 (33 transcripts), and decreased during late stage 11 (12 transcripts) (Figure 4G). See Table S2 for data and statistical analyses.

To determine whether cells expressing other Hox genes produced similar numbers of transcripts, we also counted mRNAs for *Deformed* (*Dfd*) and *Ultrabithorax* (*Ubx*) in areas of abundant transcript accumulation during stage 11 of embryogenesis. Values for these two Hox genes were similar to those found for *Scr* in PS2, with *Dfd* having an average of 92 mRNAs per cell, and *Ubx* an average of 74 per cell (Figures 4G and 4H).

Graphs plotting number of *Scr* transcripts per cell and nascent transcription strength along the anterior-posterior axis are shown in Figures 4A′–4C′ (red and green lines, respectively). Surprisingly, for PS2 cells in the stage 10 embryo, the graphs were divergent (Figure 4A′). On the other hand, in stage

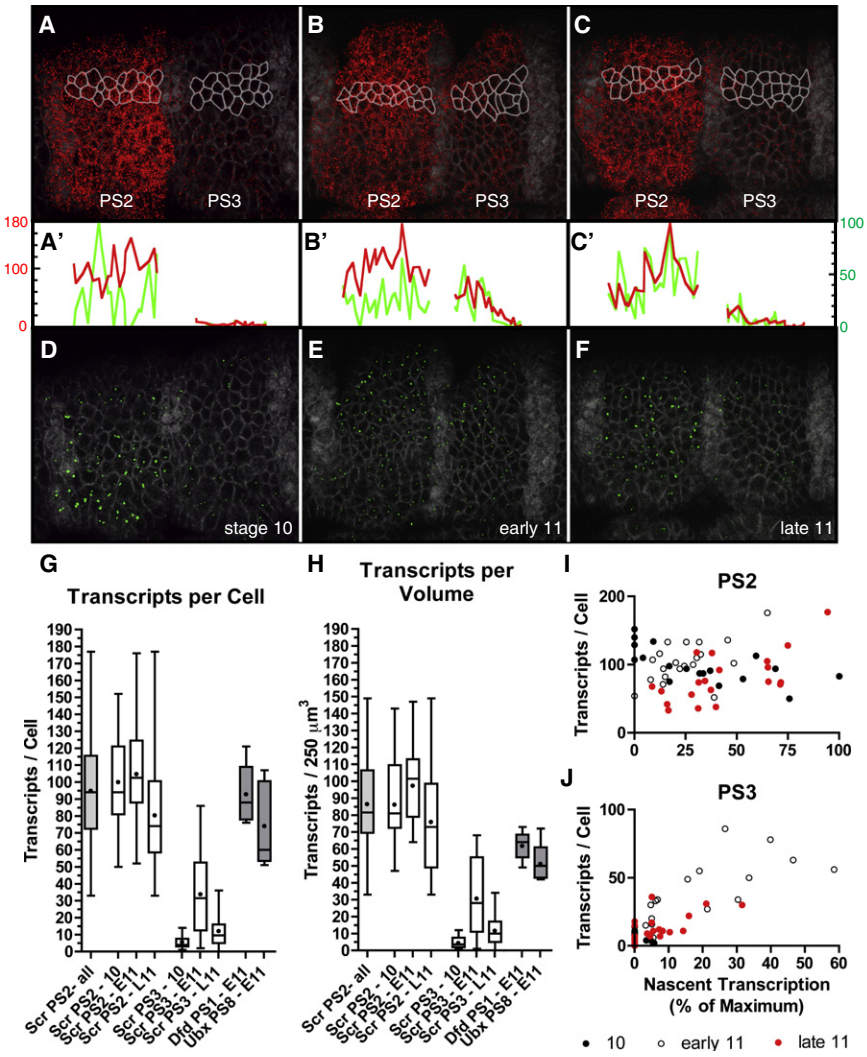

Figure 4. Analysis of *Scr* Transcription at Single-Cell Resolution

(A–C) *Scr* expression in three embryos: stage 10 (A), early stage 11 (B), and late stage 11 (C). *Scr* transcripts are shown in red, and cell membranes are marked in gray. Nuclei from the anterior compartment of each parasegment are stained for engrailed protein and appear as vertical gray stripes. The segmented cells analyzed in (G–J) are outlined in white.

(A′–C′) Graphs showing cellular transcript numbers (red lines) and relative nascent transcription strength (green line, as a percentage of the maximum value) in the outlined cells plotted against cell centroid position.

(D–F) The same embryos depicted in (A–C) stained with an intronic probe, showing sites of nascent transcription (green).

(G) Box plots summarizing transcripts per cell for various groups of cells. Boxes depict the median value and the middle two quartiles. Whiskers indicate the range of measurements, and the mean is shown as a dot inside each box.

(H) A box plot summarizing transcripts per volume (for ease of comparison to (G), values are shown with the units "transcripts/250 μm^3," which is a typical cell volume) for various groups of cells.

(I and J) Scatter diagrams plotting cellular transcript numbers against nascent transcription strength (as a percentage of maximum intensity) for PS2 and PS3 cells, respectively.

11 cells, transcript numbers and nascent transcription levels rose and fell largely in unison (Figures 4B′ and 4C′). Figures 4I and 4J show scatter plots for the cell groups in PS2 and PS3, and nonparametric correlations were calculated for all cell groups. Consistent with the traces, stage 10 PS2 cells showed a significant negative correlation between cytoplasmic transcript numbers and nascent transcription ($r = -0.7$; $p < 0.05$), whereas early and late stage 11 PS2 cell groups both showed weak but significant positive correlations ($r = 0.47$ and 0.60; $p < 0.05$) (Figure 4I). On the other hand, PS3 cells had very significant positive correlations between cellular transcript numbers and nascent transcription for both early and late stage 11 cell groups ($r = 0.85$ and 0.67 respectively; $p < 0.001$) (Figure 4J; see Table S3 for correlation data). It is possible that the same mode of transcription occurring in PS3 during stage 11 may also be occurring in PS2 during the same period, although the positive correlations are not as striking because they are superimposed upon an existing pool of transcripts.

Recent data indicates that transcription is often not only stochastic (meaning transcription initiation is probabilistic) but also occurs in bursts, during which a gene will switch back and forth between prolonged active and inactive states [2, 5, 12–16]. Our observations of large variations in transcript numbers on a cell-by-cell basis, as well as the often poor correlation between nascent transcription and cellular transcript numbers, indicate that transcriptional bursting is taking place at the *Scr* locus in PS2. One way to capture the relative intensity of these bursts is through the use of the Fano factor (FF) [16], which is essentially a measurement of population heterogeneity. In this case, it is defined as the variance of the distribution of transcript numbers per cell divided by the mean. Even stochastically transcribing cell populations can have small FF values (<1) if most cells contain similar transcript numbers, but FF values larger than 1 are suggestive of transcriptional bursting. We observed FF values of 7.1, 8.4, and 16 for the three PS2 cell groups (Table S2), which are intermediate to an observed FF value of ~4 in bacteria [12], and an FF value of >40 for a transgenic reporter gene in mammalian cells [2]. Whether the heterogeneity we observe is due to intrinsic noisiness in *Scr* transcription or to high variations in activator and repressor input (extrinsic noise) [29–32], is as yet unknown.

Our observations also indicate that there may be divergent "accumulation" and "maintenance" phases of *Scr* transcription, characterized by stage 11 PS3 cells and stage 10 PS2 cells, respectively. The *Scr* gene may begin transcribing in a stochastic, but still relatively constant manner, until a threshold number of transcripts are reached, after which it switches to a bursting mode of transcription to maintain the mRNA pool. The mechanisms whereby a cell might directly sense the concentration of a distinct mRNA species are unclear, although regulation of *Scr* transcription via downstream targets of the SCR protein could explain this phenomenon. The simultaneous RNA/protein detection procedures described in this paper should allow for more detailed studies

in which endogenous transcription factor concentrations can be correlated to target gene activity on a cell-by-cell basis.

In summary, we have characterized endogenous transcription of the *Scr* locus at single-molecule resolution in *Drosophila* embryos and have provided evidence for transcriptional bursting, as well as for two divergent modes of gene expression. To our knowledge, this is the first rigorous analysis of transcription using single-molecule FISH performed in a developing metazoan. Using FISH or live imaging in these kinds of studies is crucial, because biochemical methods that extract RNA from cell populations do not detect cell-to-cell variations. Carrying out these analyses at single-molecule resolution is similarly crucial, because metrics such as the FF are impossible to derive when using arbitrary whole-cell fluorescence measurements [16]. Finally, single-molecule measurements are much more objective and should allow for the comparison of results between disparate experiments.

Experimental Procedures

Simultaneous Fluorescent In Situ Hybridization and Protein Detection

Haptenylated probes were created by in vitro transcription, as described elsewhere [11]. The intronic probe was directly labeled with AlexaFluor 555 dyes and was prepared by Invitrogen. Simultaneous RNA and protein detection was carried out via a modified standard FISH protocol [11] with acetone used instead of Proteinase K permeabilization [10]. Dechorionated embryos were fixed in 8% formaldehyde for 25 min, devitellinized by vigorous shaking in a 1:1 heptane:methanol mixture, washed with ethanol, rocked in a 1:1 ethanol:xylenes mixture for 30 min, washed with methanol, and then gradually rehydrated in a series of methanol:H_20 washes (3:1, 1:1, 1:3, and 0:1). Embryos were permeabilized in cold 80% acetone for 10 min at −20°C, and then were transferred into phosphate buffered saline plus 0.1% Tween (PBT). Embryos were then postfixed in 5% formaldehyde in PBT for 25 min and washed with PBT. RNA probe hybridization and immunohistochemistry (including antibody combinations) were carried out as described elsewhere [11]. Spectrin [24] and engrailed [33] antibodies were obtained from the Developmental Studies Hybridoma Bank (antibodies 3A9 and 4D9, concentrate) and were used at a 1:100 dilutions.

All images were collected with a Leica SP2 laser-scanning confocal microscope. Gain and offset were set to nonsaturating levels such that intensity data would span the entire dynamic range, and line averaging was set to 2. Stacks of at least one-cell thickness (~15 μm) were collected, and channels were shifted relative to one another to correct for Z-axial chromatic aberration (which was measured independently with Tetraspeck fluorescent beads). All images were deconvolved with the AutoDeblur software program.

Cell Segmentation, Transcript Counting, and Nascent Transcription Quantification

A set of ImageJ (http://rsbweb.nih.gov/ij/) plug-ins was developed to allow us to manually segment confocal stacks (contact W. Beaver, wbeaver@cs.ucsd.edu). Transcript segmentation and counting was carried out with the image analysis program Volocity. First, transcripts were counted manually for several cells (n = 4), and this training set was used to tune the variables of the Volocity segmentation algorithm so that it predicted transcript numbers that were nearly identical to manual counts. We then used the algorithm to segment and count transcripts for the training set plus 8 more cells that were not part of the training set (Table S1). Overall the algorithm predicted values that were within ±6% of the manually derived values, and was accurate over a wide range of values (20–153) without any obvious bias toward a certain range.

Volocity was also used to measure nascent transcript intensities as well as cell volumes. Both transcribing alleles are often distinguishable, although we cannot rule out that cells containing solitary signals do not represent cases of overlapping alleles; therefore, we simply summed the intron probe fluorescence from the entire nucleus.

Supplemental Data

Supplemental data include two figures and three tables and can be found with this article online at http://www.cell.com/current-biology/supplemental/S0960-9822(09)01848-X.

Acknowledgments

We thank J. Mahaffey for providing the *Scr* cDNA plasmid, A. Hermann and A. Arvey for help with the manuscript, as well as E. Tour for troubleshooting and advice. This work was supported by National Institutes of Health (NIH) Grant HD28315 (to W.M.) and NIH Training Grant T32GM007240 (to A.P. and D.L.).

Received: July 6, 2009
Revised: September 11, 2009
Accepted: October 8, 2009
Published online: November 19, 2009

References

1. Femino, A.M., Fay, F.S., Fogarty, K., and Singer, R.H. (1998). Visualization of single RNA transcripts in situ. Science *280*, 585–590.
2. Raj, A., Peskin, C.S., Tranchina, D., Vargas, D.Y., and Tyagi, S. (2006). Stochastic mRNA synthesis in mammalian cells. PLoS Biol. *4*, e309.
3. Maamar, H., Raj, A., and Dubnau, D. (2007). Noise in gene expression determines cell fate in *Bacillus subtilis*. Science *317*, 526–529.
4. Raj, A., van den Bogaard, P., Rifkin, S.A., van Oudenaarden, A., and Tyagi, S. (2008). Imaging individual mRNA molecules using multiple singly labeled probes. Nat. Methods *5*, 877–879.
5. Zenklusen, D., Larson, D., and Singer, R. (2008). Single-RNA counting reveals alternative modes of gene expression in yeast. Nat. Struct. Mol. Biol. *15*, 1263–1271.
6. Lu, J., and Tsourkas, A. (2009). Imaging individual microRNAs in single mammalian cells in situ. Nucleic Acids Res. *37*, e100.
7. Bengtsson, M., Ståhlberg, A., Rorsman, P., and Kubista, M. (2005). Gene expression profiling in single cells from the pancreatic islets of Langerhans reveals lognormal distribution of mRNA levels. Genome Res. *15*, 1388–1392.
8. Wagatsuma, A., Sadamoto, H., Kitahashi, T., Lukowiak, K., Urano, A., and Ito, E. (2005). Determination of the exact copy numbers of particular mRNAs in a single cell by quantitative real-time RT-PCR. J. Exp. Biol. *208*, 2389–2398.
9. Warren, L., Bryder, D., Weissman, I.L., and Quake, S.R. (2006). Transcription factor profiling in individual hematopoietic progenitors by digital RT-PCR. Proc. Natl. Acad. Sci. USA *103*, 17807–17812.
10. Nagaso, H., Murata, T., Day, N., and Yokoyama, K. (2001). Simultaneous detection of RNA and protein by in situ hybridization and immunological staining. J. Histochem. Cytochem. *49*, 1177–1182.
11. Kosman, D., Mizutani, C.M., Lemons, D., Cox, W.G., McGinnis, W., and Bier, E. (2004). Multiplex detection of RNA expression in *Drosophila* embryos. Science *305*, 846.
12. Golding, I., Paulsson, J., Zawilski, S.M., and Cox, E.C. (2005). Real-time kinetics of gene activity in individual bacteria. Cell *123*, 1025–1036.
13. Chubb, J.R., Trcek, T., Shenoy, S.M., and Singer, R.H. (2006). Transcriptional pulsing of a developmental gene. Curr. Biol. *16*, 1018–1025.
14. Voss, T.C., John, S., and Hager, G.L. (2006). Single-cell analysis of glucocorticoid receptor action reveals that stochastic post-chromatin association mechanisms regulate ligand-specific transcription. Mol. Endocrinol. *20*, 2641–2655.
15. Kaern, M., Elston, T.C., Blake, W.J., and Collins, J.J. (2005). Stochasticity in gene expression: From theories to phenotypes. Nat. Rev. Genet. *6*, 451–464.
16. Raj, A., and van Oudenaarden, A. (2009). Single-molecule approaches to stochastic gene expression. Annu. Rev. Biophys. *38*, 255–270.
17. Kuroiwa, A., Kloter, U., Baumgartner, P., and Gehring, W. (1985). Cloning of the homeotic Sex combs reduced gene in *Drosophila* and in situ localization of its transcripts. EMBO J. *4*, 3757–3764.
18. Mahaffey, J.W., and Kaufman, T.C. (1987). Distribution of the Sex combs reduced gene products in *Drosophila melanogaster*. Genetics *117*, 51–60.
19. Martinez-Arias, A., Ingham, P., Scott, M., and Akam, M. (1987). The spatial and temporal deployment of Dfd and Scr transcripts throughout development of *Drosophila*. Development *100*, 673–683.
20. Fusco, D., Accornero, N., Lavoie, B., Shenoy, S., Blanchard, J., Singer, R., and Bertrand, E. (2003). Single mRNA molecules demonstrate probabilistic movement in living mammalian cells. Curr. Biol. *13*, 161–167.
21. Golding, I., and Cox, E.C. (2004). RNA dynamics in live *Escherichia coli* cells. Proc. Natl. Acad. Sci. USA *101*, 11310–11315.

22. Vargas, D.Y., Raj, A., Marras, S.A., Kramer, F.R., and Tyagi, S. (2005). Mechanism of mRNA transport in the nucleus. Proc. Natl. Acad. Sci. USA *102*, 17008–17013.
23. Lin, M.D., Jiao, X., Grima, D., Newbury, S.F., Kiledjian, M., and Chou, T.B. (2008). *Drosophila* processing bodies in oogenesis. Dev. Biol. *322*, 276–288.
24. Pesacreta, T.C., Byers, T.J., Dubreuil, R., Kiehart, D.P., and Branton, D. (1989). *Drosophila* spectrin: The membrane skeleton during embryogenesis. J. Cell Biol. *108*, 1697–1709.
25. Shermoen, A.W., and O'Farrell, P.H. (1991). Progression of the cell cycle through mitosis leads to abortion of nascent transcripts. Cell *67*, 303–310.
26. Wilkie, G.S., Shermoen, A.W., O'Farrell, P.H., and Davis, I. (1999). Transcribed genes are localized according to chromosomal position within polarized *Drosophila* embryonic nuclei. Curr. Biol. *9*, 1263–1266.
27. Boettiger, A.N., and Levine, M. (2009). Synchronous and stochastic patterns of gene activation in the *Drosophila* embryo. Science *325*, 471–473.
28. Campos-Ortega, J.A., and Hartenstein, V. (1997). The Embryonic Development of *Drosophila melanogaster*, Second Edition (Berlin, New York: Springer).
29. Elowitz, M.B., Levine, A.J., Siggia, E.D., and Swain, P.S. (2002). Stochastic gene expression in a single cell. Science *297*, 1183–1186.
30. Swain, P.S., Elowitz, M.B., and Siggia, E.D. (2002). Intrinsic and extrinsic contributions to stochasticity in gene expression. Proc. Natl. Acad. Sci. USA *99*, 12795–12800.
31. Raser, J.M., and O'Shea, E.K. (2005). Noise in gene expression: Origins, consequences, and control. Science *309*, 2010–2013.
32. Raj, A., and van Oudenaarden, A. (2008). Nature, nurture, or chance: Stochastic gene expression and its consequences. Cell *135*, 216–226.
33. Patel, N.H., Martin-Blanco, E., Coleman, K.G., Poole, S.J., Ellis, M.C., Kornberg, T.B., and Goodman, C.S. (1989). Expression of engrailed proteins in arthropods, annelids, and chordates. Cell *58*, 955–968.